Analysis of Surface Thermodynamic Characteristics within the Rear-Flank Downdraft of the Wichita, Kansas, Tornadic Supercell of 14 April 2012

Kyle Yaffe, Andrew Gordon, and Jeffrey Frame

Department of Atmospheric Sciences, University of Illinois at Urbana-Champaign

Introduction

On 14 April 2012, a long-lived supercell moved across the Wichita, KS, metropolitan area and produced an EF-3 tornado. Three Automated Surface Observing Systems (ASOS) recorded METAR observations as the storm moved overhead, with temporal resolution of up to one minute. The supercell also passed within 14 km of the KICT WSR-88D.

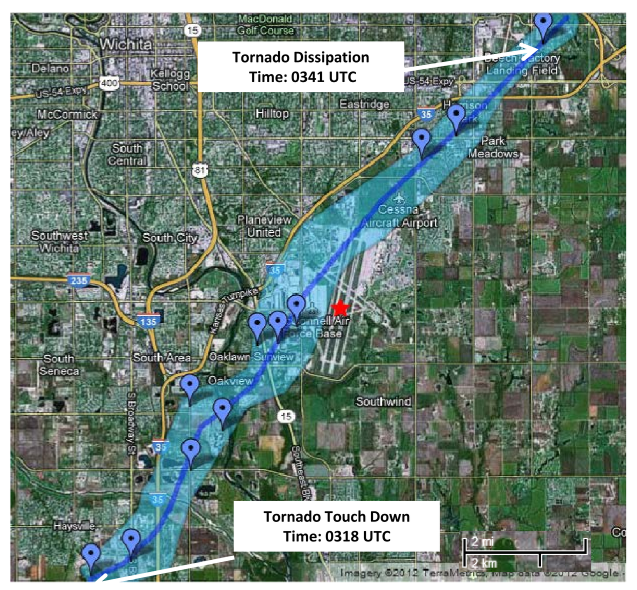

Figure 1. Map illustrating the tornado track (shaded in blue) and center line of the tornado track (heavy blue line). Location of the McConnell Air Force Base ASOS site is indicated by the red star. Map courtesy NWS Wichita.

The McConnell Air Force Base ASOS recorded wind speeds of up to 52 knots, and gusts of up to 66 knots at a distance of about 915 meters from the center of the tornado track, and about 135 meters from the edge of the tornado track. Estimated damage from this tornado is over $280 million.

This study analyzes the equivalent potential temperature (θ_e) and the virtual potential temperature (θ_v) fields within the forward-flank and rear-flank downdraft regions of the storm. This analysis will further justify the assertion that RFDs with relatively small deficits of θ_e and θ_v (i.e., relatively warmer and more potentially buoyant RFDs) are associated with a greater likelihood of long-lived intense tornadoes (e.g., Markowski et al. 2002).

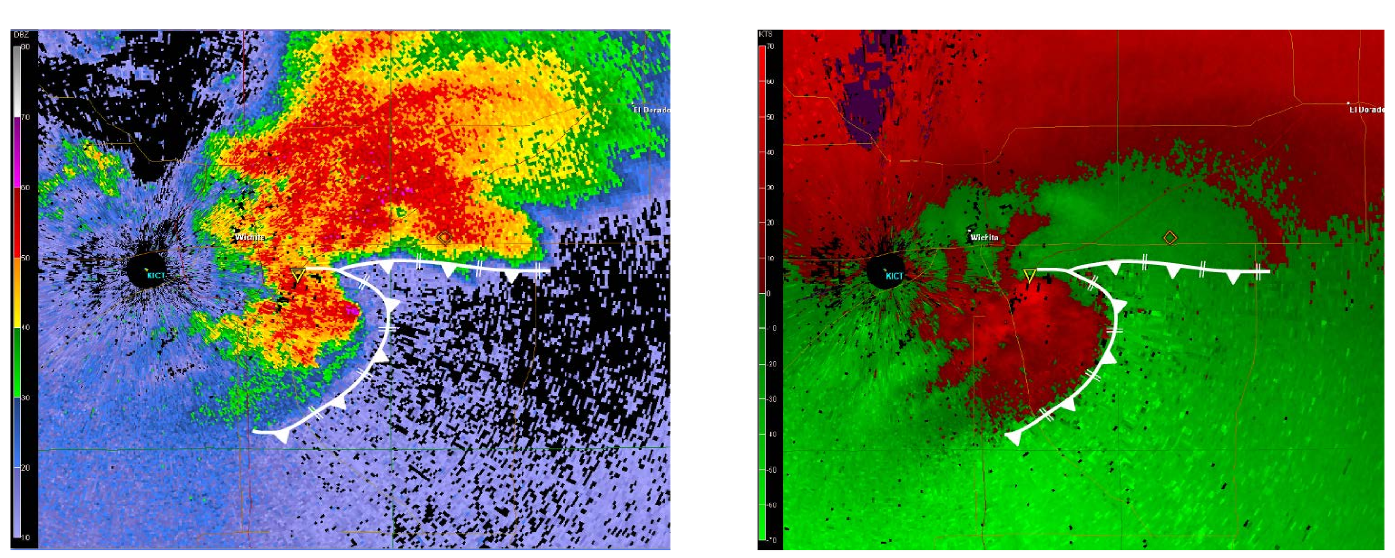

Figure 2. KICT reflectivity image (left) and radial velocity image (right) at 0331 UTC showing the locations of the forward-flank and the rear-flank gust fronts.

Methodology

From each METAR observation, the θ_e and θ_v values were determined. Storm motion vectors were calculated from the WSR-88D imagery over 12-minute intervals by tracking the low-level mesocyclone, and the thermodynamic data were plotted at their GPS-determined locations via a simple time-to-space conversion. Each image displays data collected over 24-minute periods centered on the time at which the radar data were collected.

Results

An analysis of θ_v at 0310 UTC (Fig. 3) depicts only small deficits, on the order of 1 K, within the forward flank, with larger deficits of 4-5 K near the left-rear flank of the storm. A later analysis at 0331 UTC (Fig. 4) reveals deficits of similar magnitude closer to the hook echo and tornado, on the order of 0.5-2 K. In both regions, these deficits fall within the range found for tornadic supercells by Markowski et al. (2002) and Shabbott and Markowski (2006).

$\theta_v{}'$ 0310 UTC

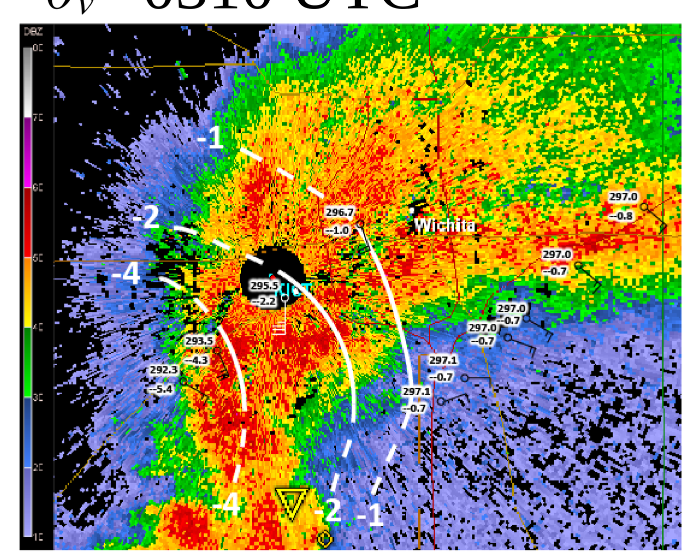

$\theta_v{}'$ 0331 UTC

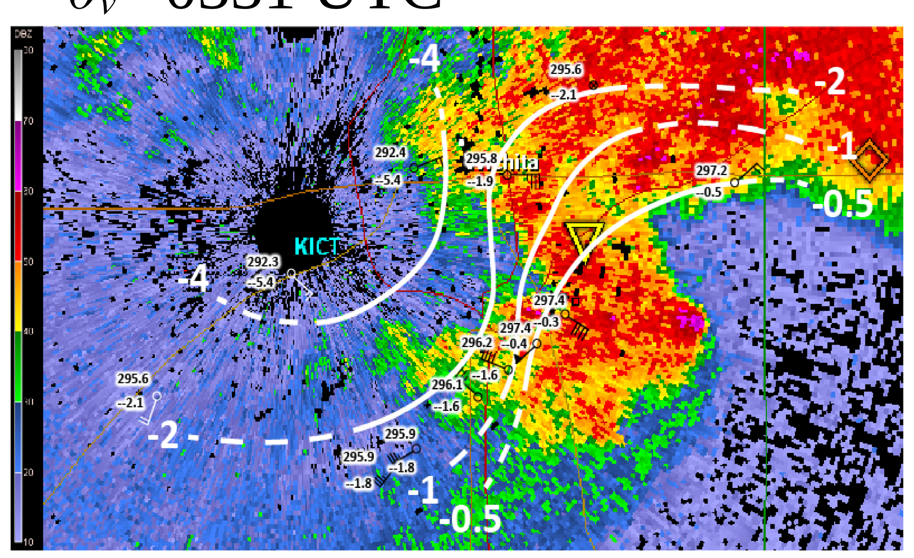

Figure 3 (left) and Figure 4 (right). KICT reflectivity images with θ_v observations superposed. On station plots, the top number is θ_v (K), and the bottom number is $\theta_v{}'$ (K) Contour lines show $\theta_v{}'$. Contours are dashed in regions where their location is less certain.

The analyses of θ_e within the forward-flank (Fig. 5), and the rear-flank downdrafts (Fig. 6), also exhibit small deficits. Deficits around 3 K are found within the FFD while the region near the tornado contains deficits of 1-2 K. These are also consistent with the findings of Markowski et al. (2002) and Shabbott and Markowski (2006).

$\theta_e{}'$ 0310 UTC

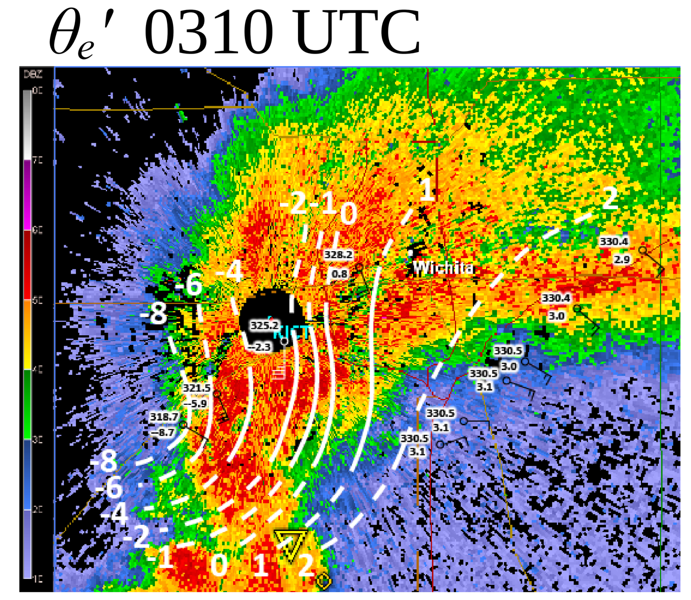

$\theta_e{}'$ 0331 UTC

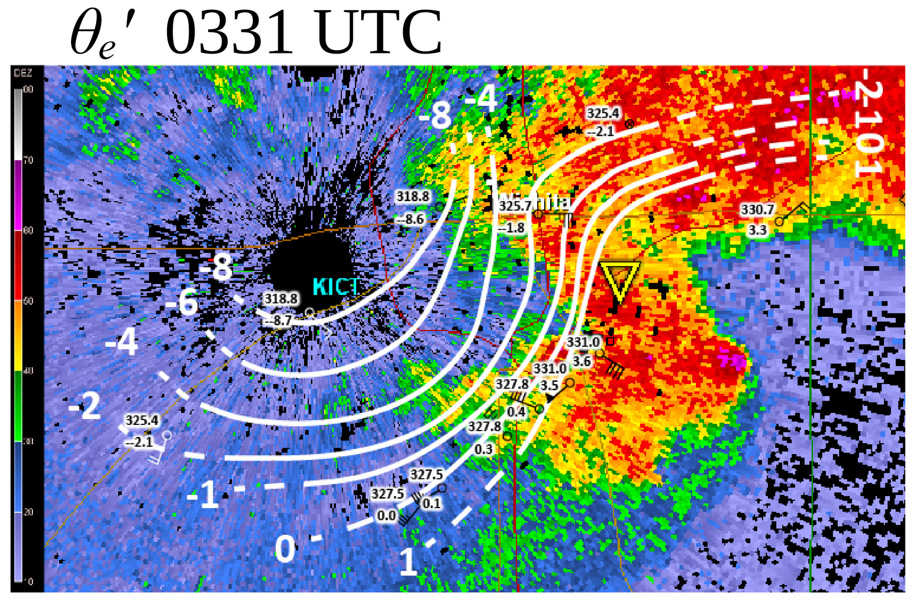

Figure 5 (left) and Figure 6 (right). KICT reflectivity images with θ_e observations superposed. On station plots, the top number is θ_e (K), and the bottom number is $\theta_e{}'$ (K) Contour lines show $\theta_e{}'$. Contours are dashed in regions where their location is less certain.

In the left-rear flank of the storm, large deficits of θ_e and θ_v, on the order of 9 K and 5 K, respectively, exist. The low-level winds indicate that this cold air was not feeding the tornado during the observation period. Unfortunately, there are no observation sites farther northeast that may confirm if the entrainment of this air into the tornado played a role in its dissipation.

Results

The region nearest the tornado is characterized by low pressure, with a minimum of 992.3 mb, and a pressure deficit of almost 7 mb relative to the near-storm environment (Fig. 7). Since this observation is outside of tornado track, we do not expect this to be representative of the minimum pressure at the center of the tornado.

p 0331 UTC

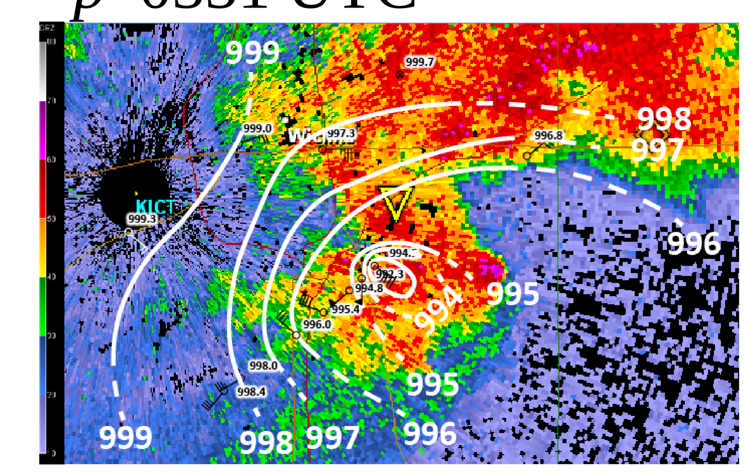

Figure 7. KICT reflectivity images with p observations superposed. Contours are dashed in regions where their location is less certain.

V_r 0331 UTC

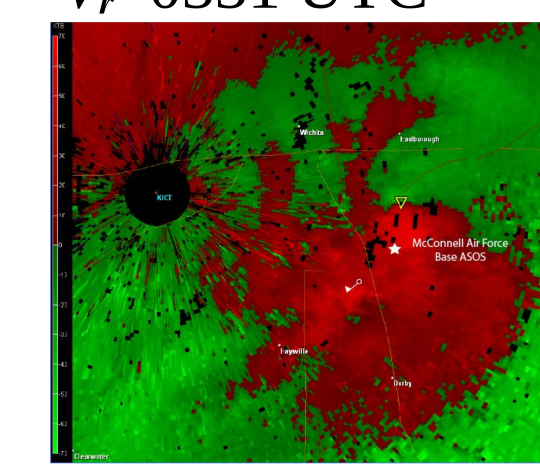

Figure 8. KICT radial velocity image at 0331 UTC. The wind observation at 0334 UTC is indicated. Location of the KIAB ASOS site is indicated by the white star.

The surface wind direction observed at 0331 UTC does not completely match that seen in the low-level radial velocity data (Fig. 8), likely because the WSR-88D beam was above the inflow layer of the tornado (175 m AGL). In the inflow layer, winds not only rotate counter-clockwise, but also exhibit a radial component toward the tornado center, which would result in a surface wind from the southwest at the ASOS site.

Conclusions and Future Work

Analyses of θ_e and θ_v provide evidence that supplements the understanding that relatively warmer and more potentially buoyant RFDs are associated with more long-lived and intense tornadoes. Future work should include analyses of:

- Surface-based convective available potential energy (CAPE) and convective inhibition (CIN)
- Storm-relative wind vectors
- More cases of both tornadic and nontornadic supercells moving in close proximity to surface observing sites
- Thermodynamic properties of the left-rear flank outflow

Acknowledgments

Zach Wienhoff, for his assistance with image manipulation.